ISSN 0036-0244, Russian Journal of Physical Chemistry A, 2022, Vol. 96, No. 10, pp. 2189–2197. © Pleiades Publishing, Ltd., 2022.
Russian Text © The Author(s), 2022, published in Zhurnal Fizicheskoi Khimii, 2022, Vol. 96, No. 10, pp. 1471–1480.

PHYSICAL CHEMISTRY
OF SURFACE PHENOMENA

Mechanism of Corrosion of Low-Carbon Steel in 1 M Solutions of Hydrochloric Acid Saturated with Oxygen

Ya. G. Avdeev[a,*] and T. E. Andreeva[a]

[a] *Frumkin Institute of Physical Chemistry and Electrochemistry, Russian Academy of Sciences, Moscow, 119071 Russia*

**e-mail: avdeevavdeev@mail.ru*

Received February 3, 2022; revised March 17, 2022; accepted March 18, 2022

Abstract—Potentiometry and voltammetry with a rotating disk electrode are used to study the corrosion of St3 low-carbon steel in 1 M HCl containing dissolved molecular oxygen from the mass loss of metal samples in a static and dynamic aggressive environment. It is shown that molecular oxygen in the acid solution and the transition from the static to dynamic state of an aggressive medium accelerates the corrosion of steel. The corrosion of steel in this environment includes the anodic ionization of steel in the kinetic region and two partial cathodic reactions: the evolution of hydrogen and the reduction of dissolved molecular oxygen, characterized by kinetic and diffusion controls, respectively. Modeling the effect the hydrodynamic mode of the motion of a corrosive medium has on the rate of the cathodic reduction of molecular O_2 on low-carbon steel using the Levich equation and comparing the results to experimental data suggests with high probability that in the flow of a corrosive medium it mainly proceeds according to the scheme $O_2 + 2H^+ + 2e = H_2O_2$. The values of the true kinetic currents of the cathodic reaction are estimated for a steel disk electrode in 1 M HCl that is freely aerated with air and forcibly aerated with gaseous O_2. The effective coefficient of diffusion of dissolved molecular O_2 in 1 M HCl is established.

Keywords: kinetics of diffusion, acid corrosion, mild steel, hydrochloric acid, reaction of oxygen reduction

DOI: 10.1134/S0036024422100041

INTRODUCTION

Solutions of mineral acids used in industry come into contact with the atmosphere, saturating them with molecular oxygen. This changes their aggressiveness in relation to steel structures that come into contact with them, as a result of its participation in the corrosion process. Most often, solutions of hydrochloric acid used in a dynamic rather than a static state are saturated with atmospheric oxygen.

In simplified form, the corrosion of low-carbon steels in solutions of mineral acids (so-called non-oxidizers) is described by the general reaction

$$2H^+ + Fe = Fe^{2+} + H_2, \quad (1)$$

which is a result of the predominant occurrence of partial reactions [1]: the anodic dissolution of iron

$$Fe - 2e = Fe^{2+}, \quad (2)$$

and the cathodic evolution of hydrogen

$$2H^+ + 2e = H_2. \quad (3)$$

Reaction (3) [1] includes the delivery of H^+ from the bulk of the acid to the metal surface ($(H^+)_*$ is the hydrogen ion closest to the metal surface)

$$H^+ \rightarrow (H^+)_*, \quad (4)$$

and the charge transfer stage (the Volmer reaction)

$$(H^+)_* + e \rightarrow H_{ad}. \quad (5)$$

This is followed by a stage of chemical (the Tafel reaction)

$$H_{ad} + H_{ad} \rightarrow (H_2)_{ad} \quad (6)$$

or electrochemical recombination (the Heyrovsky reaction)

$$H_{ad} + (H^+)_* + e \rightarrow (H_2)_{ad}. \quad (7)$$

The combination of stages (5) and (6) is called the Volmer–Tafel mechanism; (5) and (7), the Volmer–Heyrovsky mechanism. It is believed that both mechanisms operate on surfaces of steel during the evolution of hydrogen [2].

The earliest mechanism of the anodic ionization of iron, proposed by Heusler in [1], assumes that compound $FeOH_{ad}$ forms during the reaction between Fe atoms of the crystal lattice and adsorbed OH^-:

$$Fe + OH^-_{ad} \rightarrow FeOH_{ad} + e. \quad (8)$$

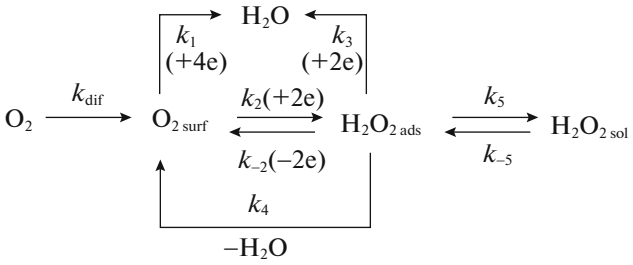

Fig. 1. Possible reactions of oxygen reduction in an acidic medium: k_{dif} is the rate constant of oxygen diffusion from the bulk of the solution to the electrode's surface, k_1 is the rate constant of oxygen reduction along the four electron pathway, k_2 and k_3 are the constants of successive stages of oxygen reduction with the formation of an intermediate particle, k_{-2} is the rate constant of hydrogen peroxide oxidation, k_4 is the constant of the chemical decomposition of hydrogen peroxide, k_5 (k_{-5}) is the rate constant of the desorption (adsorption) of hydrogen peroxide on the electrode's surface.

The subsequent transition of Fe(II) ions through the double layer is catalyzed by this compound:

$$\begin{aligned} &Fe + OH^-_{ad} + FeOH_{ad} \\ &\rightarrow (FeOH^+)_* + FeOH_{ad} + 2e. \end{aligned} \quad (9)$$

$FeOH^+$ compounds in turn decompose slowly:

$$(FeOH^+)_* + (H^+)_* \rightarrow (Fe^{2+})_* + H_2O. \quad (10)$$

In [3], Bockris considered FeOH an intermediate product in the stepwise course of the reaction

$$Fe + OH^- \rightarrow FeOH + e, \quad (11)$$

$$FeOH \rightarrow FeOH^+ + e, \quad (12)$$

$$FeOH^+ \rightarrow Fe^{2+} + OH^-. \quad (13)$$

For hydrochloric acid solutions, Chin and Nobe [4] recognized the participation of OH^- and chloride anions in the anodic reaction of iron:

$$Fe + Cl^- + H_2O \leftrightarrow [FeCl(OH)]^-_{ads} + H^+ + e, \quad (14)$$

$$[FeCl(OH)]^-_{ads} \rightarrow [FeCl(OH)] + e, \quad (15)$$

$$[FeCl(OH)] + H^+ \rightarrow Fe^{2+} + Cl^- + H_2O. \quad (16)$$

In acid solutions containing a strong oxidizing agent (molecular oxygen), two additional cathodic partial processes are thermodynamically allowed [5] with the participation of four

$$O_2 + 4H^+ + 4e = 2H_2O, \quad E^\circ = 1.229\ V \quad (17)$$

and two electrons

$$O_2 + 2H^+ + 2e = H_2O_2, \quad E^\circ = 0.70\ V. \quad (18)$$

Based on an analysis of kinetic data, Tarasevich [6] proposed a scheme for the reduction of oxygen on metals in acidic media (Fig. 1). Similar schemes were discussed in [7–9]. For an inert gold electrode, the sequential reduction of oxygen is described as

$$\begin{aligned} &O_{2\ ads} + e \leftrightarrow O^-_{2\ ads} \\ \text{or}\quad &O_{2\ ads} + H^+ + e \leftrightarrow HO_{2\ ads}, \end{aligned} \quad (19)$$

$$\begin{aligned} &O^-_{2\ ads} + e + 2H^+ \rightarrow H_2O_{2\ ads} \\ \text{or}\quad &HO_{2\ ads} + e + H^+ \rightarrow H_2O_{2\ ads}, \end{aligned} \quad (20)$$

$$H_2O_{2\ ads} + e + H^+ \leftrightarrow H_2O + OH_{ads}, \quad (21)$$

$$OH_{ads} + e + H^+ \rightarrow H_2O, \quad (22)$$

including limit stages (19) and (21) [6].

The mechanisms of the evolution of cathodic hydrogen and the anodic ionization of iron considered above are generally accepted, and their refinement is beyond the scope of the study. In contrast, the participation of molecular oxygen dissolved in acids in the corrosion of low-carbon steels was not considered in the literature available to us. Note that in solutions of mineral acids saturated with atmospheric oxygen, a transition to a passive state is possible for steels alloyed with chromium, due to the acceleration of the cathodic reaction by reducing molecular oxygen, but this effect is not observed in hydrochloric acid solutions [1].

In light of the above, it is important to establish features of the corrosion mechanism of low-carbon steel in 1 M HCl saturated with molecular oxygen.

EXPERIMENTAL

Solutions were prepared using HCl (reagent grade) and distilled water. Gaseous hydrogen and oxygen were obtained via the electrolysis of aqueous 16% NaOH (E = 2.3–2.6 V) on steel electrodes in a U-shaped glass electrolyzer. Hydrogen was additionally purified of trace amounts of oxygen by passing it through a quartz electric furnace (t = 400–600°C) filled with platinized asbestos.

The rate of corrosion of St3 low-carbon steel (composition, wt %: C, 0.14–0.22; P, 0.04; Si, 0.15–0.33; Mn, 0.40–0.65; S, 0.05; Cr, 0.3; Ni, 0.3; N, 0.008; Cu, 0.3; As, 0.08; the remainder, Fe) in 1 M HCl at t = 25°C was determined from the mass loss of samples (≥4 per point) 50 × 20 × 3.0 mm^3 in size, at a rate of 50 mL of acid solution per sample:

$$k = \Delta m S^{-1} \tau^{-1}, \quad (23)$$

where Δm is the change in the mass of the sample, g; S is the sample area, m^2; and τ is the duration of corrosion tests, h. Each experiment was 2 h long. Before an experiment, the samples were cleaned on an abrasive wheel (ISO 9001; grit size, 60) and degreased with

Table 1. Rate of corrosion (k), increment of corrosion loss (Δk), and corrosion acceleration factor (γ^{-1}) of St3 steel in 1 M HCl deaerated with hydrogen and aerated with oxygen, k and Δk in g/(m^2 h). The duration of each experiment is 2 h, t = 25°C, and v is the flow rate of the solution

v, m/s	Solution deaerated with $H_{2(g)}$			Solution aerated with $O_{2(g)}$			Δk**	γ^{-1}**
	k	Δk*	γ^{-1}*	k	Δk*	γ^{-1}*		
0	3	—	—	5	—	—	2	1.7
0.5	3	0	1.0	12	7	2.4	9	4.0
1.0	3	0	1.0	19	14	3.8	16	6.3
1.5	3	0	1.0	21	16	4.2	18	7.0
2.0	3	0	1.0	23	18	4.6	20	7.7
2.5	3	0	1.0	23	18	4.6	20	7.7

* Change in value as a result of acceleration of the flow of the solution.

** Change in value as a result of O_2 in the solution.

acetone. Our studies were performed in a glass circulation cell with a propeller stirrer at a corrosive medium flow rate of 0–2.5 m/s. Corrosive media were deaerated with gaseous hydrogen (p = 1 atm) or forcedly aerated with gaseous oxygen (p = 1 atm) for 2 h before an experiment and during corrosion tests of the samples.

The effects of the oxygen dissolved in the acid and the nature of the flow of the corrosive medium on the rate of steel corrosion was estimated from the increment of corrosion losses

$$\Delta k = k_{O_2} - k_0, \quad (24)$$

$$\Delta k = k_{dyn} - k_{st}, \quad (25)$$

and the coefficient of corrosion acceleration

$$\gamma^{-1} = k_{O_2} k_0^{-1},$$

$$\gamma^{-1} = k_{dyn} k_{st}^{-1},$$

where k_{O_2} and k_0 are the rates of steel corrosion in acid solutions forcedly aerated by oxygen and deaerated, and k_{dyn} and k_{st} are the rates of corrosion in dynamic and static media.

Electrochemical measurements were made using a P-5827M potentiostat with a rotating disk electrode made of St3 steel (460 rpm) in 1 M HCl deaerated with hydrogen, freely aerated with air, and forcedly aerated with oxygen at t = 25°C. The steel electrode was cleaned with M20 sandpaper and degreased with acetone. Steel potentials were measured relative to a silver chloride electrode. Our studies were performed using a hermetically sealed glass electrochemical cell with an external space for silver chloride and auxiliary platinum (0.5 cm^2) electrodes. Potentiometric studies were performed using a two-electrode scheme (working steel and silver chloride electrodes). Voltammetric studies were performed according to a three-electrode scheme in the potentiodynamic mode at a working electrode polarization rate of 0.0005 V/s. Prior to polarization, the electrode was kept in the test solution for 30 min to establish free corrosion potential E_{cor}. The curves of the anodic and cathodic polarization of the steel were then recorded. The effect the convective factor had on the rate of the cathodic reaction of steel was measure at E = −0.30 and −0.35 V for disk electrode rotation speeds n = 0, 460, 780, 1090, 1400 rpm.

The effect the dissolved oxygen had on the electrode reactions of steel was estimated from the values of the coefficient of acceleration:

$$\gamma^{-1} = i_{O_2} i_0^{-1}, \quad (26)$$

where i_0 and i_{O_2} are the current densities in deaerated and oxygenated acid solutions.

The values of the electrode potentials are given according to the standard hydrogen scale.

RESULTS AND DISCUSSION

The corrosion of low-carbon steel in 1 M HCl deaerated with hydrogen proceeded at a relatively low rate that did not depend on the hydrodynamic regime of the medium (Table 1). In contrast, the dissolved O_2 (p = 1 atm) in the corrosive medium strongly accelerated the corrosion of steel. The increase in corrosion losses due to the O_2 in an aggressive environment was 2–20 g/(m^2 h) depending on the flow rate of the acid solution. The faster the flow of the liquid medium, the higher the value of Δk. Because of the oxidizing agent, the increment of corrosion losses in the flow of the medium is in all cases greater than the rate of corrosion under static conditions. In 1 M HCl saturated with O_2, steel corrosion grew along with the flow rate of the aggressive medium, which is typical of processes with diffusion control. It is important that the highest flow rate (2.5 m/s) in the deaerated solution of steel, k was 3 g/(m^2 h). In the solution aerated with O_2, it was 23 g/(m^2 h), though the content of dissolved O_2 in the

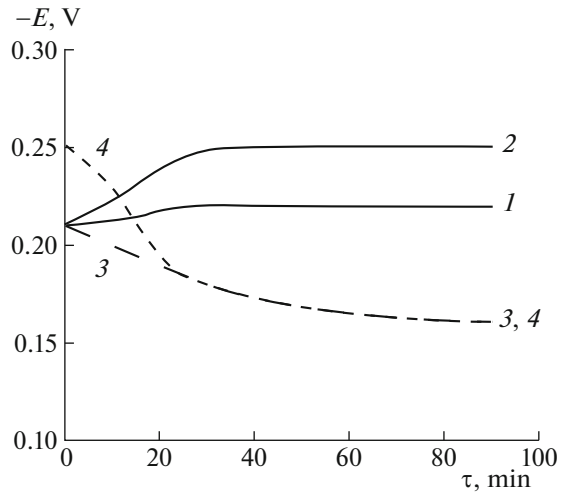

Fig. 2. Corrosion potentials of steel St3 (*1*) in freely aerated 1 M HCl (*2*) after switching on deaeration with H_2 gas and (*3*) aeration with O_2 gas. Line *4* shows the corrosion potentials of steel in deaerated 1 M HCl after switching on aeration with gaseous O_2; n = 460 rpm, t = 25°C.

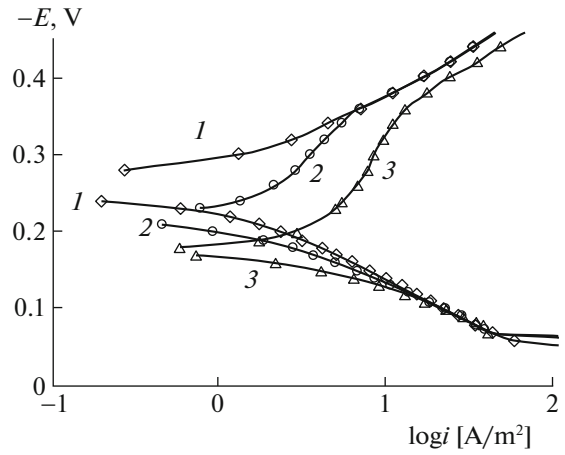

Fig. 3. Polarization curves of St3 steel in 1 M HCl (*1*) deaerated with gaseous H_2, (*2*) freely aerated with air, and (*3*) forcibly aerated with gaseous O_2; n = 460 rpm, t = 25°C.

corrosive medium was much lower than the content of HCl.

Substantial acceleration of corrosion of low-carbon steel in HCl with dissolved O_2 was thus shown. The rate of steel corrosion in the environment aerated with O_2 depended on the intensity of its flow, which is typical of processes with diffusion control. More detailed information about the effect dissolved O_2 had on the corrosion of steels in acid solutions can be obtained using electrochemical means to study the corrosion system: potentiometry and voltammetry, along with studying the effect hydrodynamic parameters have on electrode processes using a rotating disk electrode.

Deaeration of a 1 M HCl solution with gaseous H_2 shifted the free corrosion potential of steel (E_{cor}) to lower potentials (Fig. 2). Allowing for the chemical composition of the corrosive medium, this could be a result of the cathodic reaction slowing due to the removal of O_2. In contrast, preliminarily deaerated or freely aerated 1 M HCl with forced aeration with oxygen, raises the E_{cor} of steel, due to the increased content of O_2 in the aggressive environment accelerating the cathodic reaction. It is important that the E_{cor} values of steel are in the region of active dissolution of the metal in both the deaerated HCl solution and the aerated (p_{O_2} = 0.2 and 1 atm) solutions.

The nature of the polarization curves (PC) of low-carbon steel in 1 M HCl testifies to the corrosion of the metal in the region of active dissolution (Fig. 3, Table 2). In 1 M HCl, the slope of the cathodic polarization of steel (b_c) is close to the theoretically predicted value of 0.115 V; in contrast, the slope of the anodic polarization of steel (b_a) is higher than the theoretical value of 0.070 V [10]. The increase in slope b_a of steel is a result of the formation of a layer of sludge on its surface during the dissolution of the metal, as was observed visually.

The dissolved O_2 in 1 M HCl shifted the free corrosion potential of steel to more positive potentials, a result of this additive accelerating the cathode process. The higher the content of O_2 in the solution, the stronger this effect. Dissolved O_2 had virtually no effect on the anodic reaction, but the cathodic reaction was

Table 2. Corrosion potentials (E_{cor}) of St3 steel in 1 M HCl (25°C), Tafel slopes of polarization curves (b_c and b_a), cathode and anode current densities (i_c and i_a), and cathode and anode reaction acceleration factors (γ_c^{-1} and γ_a^{-1}) at E = −0.30 and −0.10 V, respectively

Experimental conditions	$-E_{cor}$	b_c	i_c	γ_c^{-1}	b_a	i_a	γ_a^{-1}
Deaerated with $H_{2(g)}$	0.25	0.12	1.31	—	0.10	22.1	—
Freely aerated	0.22	i_{lim}	3.46	2.6	0.10	22.6	1.0
Aerated with $O_{2(g)}$	0.18	i_{lim}	8.46	6.5	0.10	22.6	1.0

E in V, i in A/m^2, n = 460 rpm, t = 25°C, i_{lim} is the limit current.

Table 3. Constants i_k and f in the equation $i_c = i_k + fn^{1/2}$ at $E = -0.30$ and -0.35 V and the effective coefficients of diffusion of oxygen molecules (D) for the cathodic reaction of a steel rotating disk electrode in 1 M HCl

Experimental conditions	$E = -0.30$ V			$E = -0.35$ V		
	i_k	f	$D \times 10^{-3}$	i_k	f	$D \times 10^{-3}$
Deaerated with $H_{2(g)}$	1.81	0	—	5.77	0	—
Freely aerated	1.81	0.10	1.1 ± 0.1	5.77	0.10	1.1 ± 0.1
Aerated with $O_{2(g)}$	1.81	0.49		5.77	0.49	

i_k in A/m^2, f in A/(m^2 rpm$^{1/2}$), D in μm^2/s, $t = 25$°C.

positive in terms of concentration. The initial section of the cathode PC was characterized by the limit current (i_{lim}). In contrast, the slope of the anode polarization corresponded to the background's.

The molecular O_2 in the HCl solution had almost no effect on the nature of the anodic reaction. It proceeded according to Eq. (2) with an without it. In contrast, the nature of the cathodic PC testifies to the participation of O_2 in the cathodic reaction. In concentrated acid solutions (pH <2), the cathodic reaction corresponding to Eq. (3) proceeded in the region of kinetic control [11], which is in good agreement with the nature of the cathodic PCs we obtained. With dissolved O_2, they were complicated by the limit current, indicating a change in the mechanism of the cathodic reaction. The observed limit current was most likely due to restrictions on diffusion associated with the delivery of oxidizers in the medium to the steel surface. There were two such oxidizing agents, H^+ and O_2, but the concentration of the former in the corrosive medium was three orders of magnitude higher than that of the latter. The limit current must then be a result of diffusion limitations in the delivery of O_2 molecules to the steel surface. This assumption can be confirmed by studying the effect the flow of the electrolyte had on the rate of the cathodic reaction. The traditional solution to such an experimental problem in performing electrochemical studies is to use a disk electrode, since changing its frequency of rotation regulates the flow of the electrolyte near the metal electrode [11].

Let us assume that two independent reactions H^+, described by Eq. (3), and the reduction of O_2, described by Eqs. (17) and/or (18), proceed on steel in the region of cathodic potentials. The cathode current is then the sum of two partial currents that are difficult to separate. However, when one of reactions (3) proceeds in the kinetic region, and (17) and (18) occur in the region of diffusion, we can use the equation

$$i_c = i_k + i_d, \quad (27)$$

where i_k and i_d are the densities of the kinetic and diffusion currents. With laminar motion of the fluid near the surface of a rotating metal disk, the value of i_d is directly proportional to the square root of the rotational speed of the disk electrode (n). Expression (27) then takes the form

$$i_c = i_k + fn^{1/2}. \quad (28)$$

In 1 M HCl, the experimental dependence of i_c on $n^{1/2}$ has a linear form at different cathode E when there is free aeration with air and forced aeration of O_2 (Fig. 4, Table 3). In a deaerated acid solution, there is no response of the cathode current to a change in the rotational speed of the steel disk, confirming the kinetic nature of reaction (3). With molecular O_2, the kinetic component of the cathode current is the same as without it. This supports our assumption about the independence of the H^+ and O_2 reduction reactions. It is also clear that reaction (3) proceeds in the kinetic region, while reactions (17) and/or (18) occur in the region of diffusion. Despite the lower content of molecular O_2 in solutions relative to the acid itself, $i_k < i_d$ in a medium aerated with oxygen, even at the lowest frequency of electrode rotation (Table 4). In a freely aerated solution, $i_k > i_d$ when $E = -0.35$ V. However, $i_k < i_d$ when $E = -0.30$ V. Direct measurements of the flowing currents are not possible when steel is corroded at E_{cor}. Judging from the above data, the predominance of the reduction of molecular O_2 over that of H^+ is even stronger at E_{cor}, generally determining the overall corrosion process.

It is important to understand which process is responsible for the cathodic diffusion current: reaction (17) or/and (18). This problem can be solved by comparing experimental values of i_d and values of i_d calculated using the Levich equation [11] for four and two electronic reactions (17) and (18). This approach was

Table 4. Values of kinetic (i_k) and diffusion (i_d) partial cathode currents of the steel disk electrode in 1 M HCl

Experimental conditions	$E = -0.30$ V		$E = -0.35$ V	
	i_k	i_d	i_k	i_d
Deaerated with $H_{2(g)}$	1.81	0	5.77	0
Freely aerated	1.81	2.30	5.77	2.20
Aerated with $O_{2(g)}$	1.81	11.2	5.77	10.6

$n = 460$ rpm, i_k and i_d in A/m^2, $t = 25$°C.

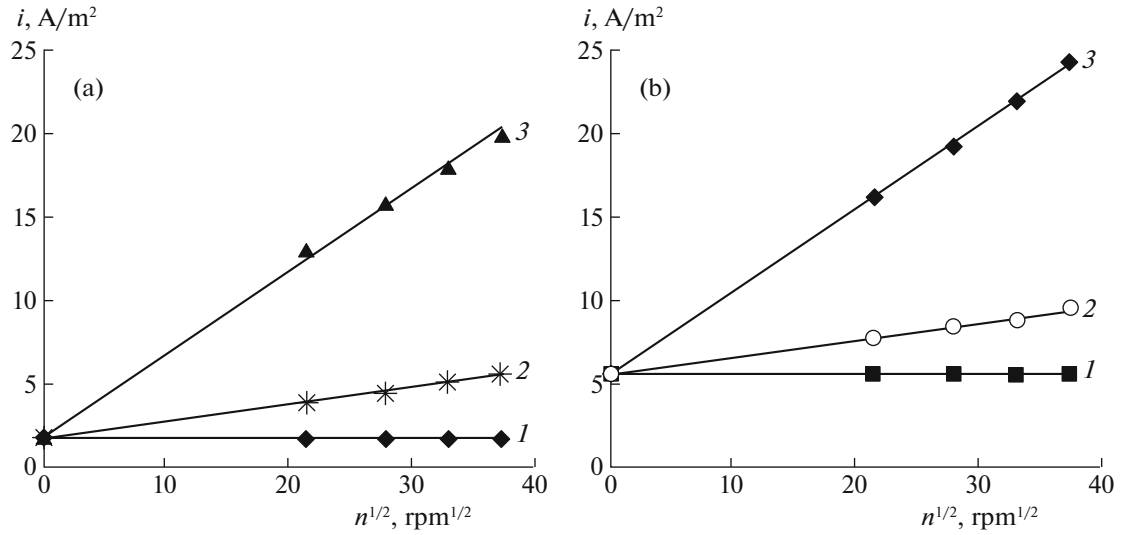

Fig. 4. Dependences of the cathode current density on the rotational speed of the St3 steel disk in 1 M HCl deaerated with gaseous H_2 (*1*), freely aerated with air (*2*), and forcibly aerated with gaseous O_2 (*3*). $E = -0.30$ (a) and -0.35 (b) C, $t = 25$°C.

used in [12] to refine the path of O_2 reduction on an electrode with encapsulated Pt nanoparticles in 0.10 M $HClO_4$, platinum in 0.1 M $HClO_4$ [13], and copper in 0.1 M KNO_3 [14]. The diffusion current resulting from the reduction of molecular O_2 on a steel cathode in a laminar flow of liquid is described by the Levich equation

$$i_d = 0.62zFC^*D^{2/3}\eta^{-1/6}n^{1/2}, \quad (29)$$

where z is the number of electrons participating in the reaction on the electrode, F is the Faraday number, C^* is the concentration of molecular O_2 in the depth of the solution, D is the coefficient of diffusion of an electroactive particle, η is the kinematic viscosity of the liquid, and n is the angular velocity of disk rotation. When calculating the theoretical values of i_d using the Levich equation (Fig. 5), we used values of η, $C(O_2)$, and D taken from different literature sources (Table 5). There were no reference data on the value of D for molecular O_2 in 1 M HCl, so we used D values for it in an aqueous medium and 0.5 M H_2SO_4 (a solution with an active acid concentration corresponding to 1 M HCl) when calculating i_d. We can that in all cases, the theoretical values of i_d are higher than the experimental ones. This indicates that in our system, i_d should be determined mainly by reaction (18) in the flow of an aggressive medium. The experimentally measured currents are in this case lower than those calculated for the two-electron reaction. The observed effect is largely due to the slowing of O_2 reduction as a result of the metal surface being screened by the evolving gaseous hydrogen. The region of reaction (18) calculated for the reference $D(O_2)$ values used for pure water is in this case farther from the experimental points than the theoretical straight line calculated for the $D(O_2)$ value used for 0.5 M H_2SO_4. This suggests that the $D(O_2)$ values are reduced in 1 M HCl, compared to pure water. A similar effect is observed not only in 0.5 M H_2SO_4, but in 1 M NaCl as well (Table 5).

The reduction of molecular O_2 on steel proceeding according to reaction (18), is not unique in a flow of a corrosive medium. Such a process can proceed on an electrode with encapsulated Pt nanoparticles in

Table 5. Viscosity of 1 M HCl solution (η), content of oxygen in water and 1 M HCl ($C(O_2)$), and coefficient of diffusion for oxygen (D)

Experimental conditions	η	$C(O_2)$		$D \times 10^{-3}$
		water	1 M HCl	
Freely aerated	0.0106 [15]	0.260 [16, 17]	0.247*	1.9–2.3 (water) [16]
Aerated with $O_{2(g)}$		1.22 [16]	1.16*	1.4 (0.5 M H_2SO_4) [16] 1.75 (1 M NaCl) [19]

η in cm^2/s, C in mM, D in $\mu m^2/s$, $t = 25$°C, the asterisk marks the values calculated based on the solubility of oxygen in water, allowing for the correction factor ($\phi = 0.95$) taken from [18].

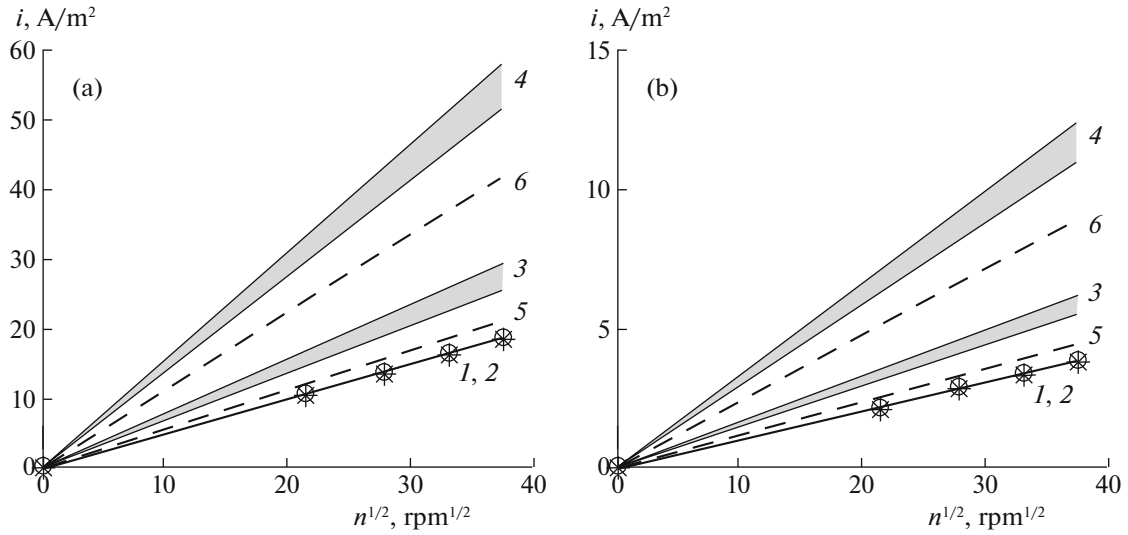

Fig. 5. Dependences of the diffusion current density on the rotational speed of the St3 steel disk in 1 M HCl (a) forcibly aerated with gaseous O_2 and (b) freely aerated with air. (*1*, *2*) Experimental data at $E = -0.30$ and -0.35 V; (*3*) model for two-electron reaction (18); (*4*) model for four electron reaction (17); (*5*) model for two electron reaction (18) at 0.5 M H_2SO_4; (*6*) model for four electron reaction (17) in 0.5 M H_2SO_4 at $t = 25$°C.

0.10 M $HClO_4$ [12] and a copper electrode in 0.1 M KNO_3 [14]. This shows that the higher rates of mass transfer of molecular oxygen achieved by increasing the rotation of the disk metal electrode transforms the process from a four-electrode to a two-electron reaction. Note that Dumitrescu and Crooks [12] neither considered the effect to be a consequence of a change in the path from reaction (17) to (18) nor provide a convincing explanation for it. It is assumed that due to the high speed of the aggressive medium, some of the O_2 molecules flow past the electrode's surface with the liquid and do not have time to recover.

The reaction of O_2 reduction in solutions of mineral acids is normally studied on inert metals where there is no parallel proton reduction reaction. Both processes occurred in our system, complicating its experimental study and making it difficult to obtain the true kinetic parameters of the process. The most harmful process in this respect was the release of gaseous hydrogen on the steel electrode, partially shielding the metal surface from the aggressive environment. Our data allowed us to calculate the effective parameters of the system, but it was assumed they would be close to the true values.

Based on the above, we can calculate the effective $D(O_2)$ values for 1 M HCl, determined from data on the effect the speed of the steel disk's rotation had on the cathode current. In our calculations, we assumed the reduction of O_2 on steel proceeds according to reaction (18). The resulting effective value of $D(O_2)$ was close to 1.1×10^3 μm²/s, regardless of the value of E for steel (Table 3).

Another way of obtaining information on the effect the convective factor has on the rate of electrode reactions is to analyze the dependence of $1/i$ on $1/n^{0.5}$, which is described by the equation [11, 20–22]

$$\frac{1}{i} = \frac{1}{i_\infty} + K\frac{1}{n^{1/2}},$$

where i_∞ is the value of the true kinetic current, and K is a proportionality factor depending on η and D. Extrapolating linear dependence $1/i$ from $1/n^{0.5}$ to $n \to \infty$ (i.e., $1/n^{0.5} \to 0$) allows us to determine the true kinetic current, which expresses the rate of the reaction at a concentration of reactants unchanged by the passage of an electric current. Establishing the values of the true kinetic current is one that of determining the value of the reaction rate constant directly. Since two particles were depolarizers in our system, it is not possible to solve such a problem. Even so, it is important to analyze the effect molecular O_2 has on this quantity (Fig. 6, Table 6). In 1 M HCl with no dissolved O_2, the values of i_c correspond to i_∞, which is typical of a process proceeding with kinetic control. In contrast, $i_c < i_\infty$ when there is molecular O_2 in these solutions. The higher the content of in the solution, the higher the observed values of i_∞. In solutions containing O_2, lowering the E of the steel electrode increases i_∞, due primarily the result to an increase in the rate of H^+ reduction.

In this work, we considered the direct effect dissolved molecular O_2 has on the corrosion of low-carbon steel in 1 M HCl when this oxidizing agent participates directly in the cathodic process. Another indirect path is also possible. The products of steel

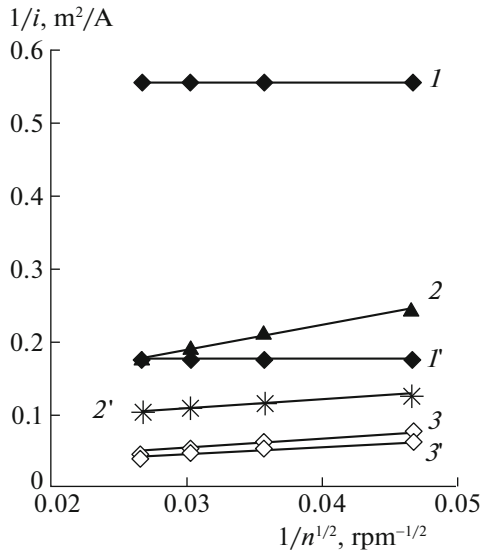

Fig. 6. Dependences of the reciprocal density of the cathode current on the reciprocal square root of the frequency of rotation of the St3 steel disk in 1 M HCl deaerated with gaseous H_2 (*1*, *1'*), freely aerated with air (*2*, *2'*), and forcibly aerated with gaseous O_2 (*3*, *3'*); (*1*, *2*, *3*) $E = -0.30$ V and (*1'*, *2'*, *3'*) $E = -0.35$ V, $t = 25$°C.

corrosion in an acidic environment are Fe(II) salts. Over time, they accumulate in the corrosive environment. Molecular O_2 dissolved in it can oxidize the Fe(II) salts, converting them into Fe(III) salts. The kinetic patterns of the oxidation of Fe(II) salts in an acid solution with dissolved O_2 were discussed in [23, 24]. Another oxidizing agent appears in the system that is capable of participating in the corrosion process. We considered the mechanism of corrosion of steels in acids containing Fe(III) salts in [25, 26].

Reasons for the acceleration of corrosion of mild steel in 1 M HCl with molecular O_2 were thus established. Molecular O_2 in an aggressive environment participates in the corrosion process as an additional oxidizing agent. In this system, corrosion consists of three partial reactions of the anodic ionization of iron and cathodic reduction of protons proceeding with kinetic control, along with the cathodic reduction of O_2 determined by kinetics of diffusion. A similar pattern of the corrosion of low-carbon steels in solutions of mineral acids is observed when using an oxidizing agent like Fe(III) salts in an aggressive medium [25, 26]. Our result is important in theoretical terms, since it expands our understanding of the steel corrosion mechanism in air-aerated solutions of mineral acids. It is also interesting from a practical point of view, since industrial acid solutions are freely aerated by air. In such environments, the corrosion of low-carbon steels will proceed with a considerable proportion of oxygen depolarization, especially in dynamic systems. Unfortunately, this is usually ignored in works on the acid corrosion of low-carbon steels.

Table 6. Effective values of the true kinetic currents of the cathodic reaction (i_∞) for the steel disk electrode in 1 M HCl

Experimental conditions	$E = -0.30$ V	$E = -0.35$ V
Deaerated with $H_{2(g)}$	1.81	5.77
Freely aerated	11	13
Aerated with $O_{2(g)}$	65	67

i in A/m^2, $t = 25$°C.

CONCLUSIONS

1. We demonstrated the accelerating effect dissolved molecular O_2 has on the corrosion of mild steel in 1 M HCl. The greater the flow rate of the liquid aggressive medium, the stronger the effect dissolved O_2 has on the corrosion of steel, which is typical of processes with diffusion control.

2. The corrosion of mild steel in 1 M HCl containing dissolved O_2 includes an anodic ionization reaction of metallic iron occurring in the kinetic region. The cathodic reaction combines the parallel and independent evolution of hydrogen with kinetic control, while the reduction of molecular O_2 is characterized by diffusion control.

3. Analysis of the effect the convective factor has on the cathodic reduction of O_2 on low-carbon steel in 1 M HCl using the Levich equation suggests that in the flow of an aggressive medium, it mainly proceeds according to the scheme

$$O_2 + 2H^+ + 2e = H_2O_2.$$

4. Kinetic parameters of the cathodic reaction of steel in 1M HCl containing molecular O_2 were established. The effective coefficient of diffusion of dissolved molecular O_2 in 1 M HCl was determined. The true currents of the cathodic reaction on a steel electrode in a 1 M HCl solution aerated freely with air and forced with gaseous O_2 were calculated.

FUNDING

This work was supported by R&D 2022–2024 "Chemical Resistance of Materials: Protecting Metals and Other Materials from Corrosion and Oxidation," EGISU registration no. 122011300078-1, inventory number FFZS-2022-0013.

REFERENCES

1. H. Kaesche, *Die Korrosion der Metalle. Physikalisch-chemische Prinzipien und aktuelle Probleme* (Springer, Berlin, 1979).
2. L. I. Antropov, *Theoretical Electrochemistry* (Vyssh. Shkola, Moscow, 1965), p. 348 [in Russian].

3. J. O. Bockris, D. Drazic, and A. R. Despic, Electrochim. Acta **4**, 325 (1961). https://doi.org/10.1016/0013-4686(61)80026-1
4. R. J. Chin and K. Nobe, J. Electrochem. Soc. **119**, 1457 (1972). https://doi.org/10.1149/1.2404023
5. F. Si, Y. Zhang, L. Yan, et al., *Rotating Electrode Methods and Oxygen Reduction Electrocatalysts,* Ed. by W. Xing, G. Yin, and J. Zhang (Elsevier, Amsterdam, 2014), p. 133. https://doi.org/10.1016/B978-0-444-63278-4.00004-5
6. V. M. Andoralov, M. R. Tarasevich, and O. V. Tripachev, Russ. J. Electrochem. **47**, 1327 (2011). https://doi.org/10.1134/S1023193511120020
7. Z. Zhao and P. K. Shen, *Electrochemical Oxygen Reduction,* Ed. by P. K. Shen (Springer, Singapore, 2021), p. 11. https://doi.org/10.1007/978-981-33-6077-8_2
8. L. Vracar, *Encyclopedia of Applied Electrochemistry,* Ed. by G. Kreysa, K. Ota, and R. F. Savinell (Springer Science, New York, 2014), p. 1485.
9. Z. Jia, G. Yin, and J. Zhang, in *Rotating Electrode Methods and Oxygen Reduction Electrocatalysts,* Ed. by W. Xing, J. Zhang, and G. Yin (Elsevier, Amsterdam, 2014), p. 199. https://doi.org/10.1016/B978-0-444-63278-4.00006-9
10. Ya. G. Avdeev, K. L. Anfilov, and Yu. I. Kuznetsov, Int. J. Corros. Scale Inhib. **10**, 1566 (2021). https://doi.org/10.17675/2305-6894-2021-10-4-12
11. Yu. V. Pleskov and V. Yu. Filinovskii, *The Rotating Disk Electrode* (Consultants Bureau, New York, 1976).
12. I. Dumitrescu and R. M. Crooks, Proc. Natl. Acad. Sci. U. S. A. **109**, 11493 (2012). https://doi.org/10.1073/pnas.1201370109
13. C. Du, Q. Tan, G. Yin, and J. Zhang, in *Rotating Electrode Methods and Oxygen Reduction Electrocatalysts,* Ed. by W. Xing, G. Yin, and J. Zhang (Elsevier, Amsterdam, 2014), p. 171. https://doi.org/10.1016/B978-0-444-63278-4.00005-7
14. A. L. Colley, J. V. Macpherson, and P. R. Unwin, Electrochem. Commun. **10**, 1334 (2008). https://doi.org/10.1016/j.elecom.2008.06.032
15. Short Handbook of Physical Chemical Values, Ed. by K. P. Mishchenko and A. A. Ravdel' (Khimiya, Leningrad, 1967), p. 103 [in Russian].
16. W. Xing, M. Yin, Q. Lv, et al., in *Rotating Electrode Methods and Oxygen Reduction Electrocatalysts,* Ed. by W. Xing, J. Zhang, and G. Yin (Elsevier, Amsterdam, 2014), p. 1. https://doi.org/10.1016/B978-0-444-63278-4.00001-X
17. N. A. Mel'nichenko, Russ. J. Phys. Chem. A **82**, 1533 (2008). https://doi.org/10.1134/S0036024408090239
18. D. Tromans, Hydrometallurgy **50**, 279 (1998). https://doi.org/10.1016/S0304-386X(98)00060-7
19. G. W. Hung and R. H. Dinius, J. Chem. Eng. Data **17**, 449 (1972). https://doi.org/10.1021/je60055a001
20. A. N. Frumkin and E. A. Aikazyan, Dokl. Akad. Nauk SSSR **100**, 315 (1955).
21. A. N. Frumkin and G. A. Tedoradze, Dokl. Akad. Nauk SSSR **118**, 530 (1958).
22. X. Wang, Z. Li, Y. Qu, et al., Chemistry **5**, 1486 (2019). https://doi.org/10.1016/j.chempr.2019.03.002
23. W. N. Wermink and G. F. Versteeg, Ind. Eng. Chem. Res. **56**, 3775 (2017). https://doi.org/10.1021/acs.iecr.6b04606
24. W. N. Wermink and G. F. Versteeg, Ind. Eng. Chem. Res. **56**, 3789 (2017). https://doi.org/10.1021/acs.iecr.6b04641
25. Ya. G. Avdeev and T. E. Andreeva, Russ. J. Phys. Chem. A **95**, 1128 (2021). https://doi.org/10.1134/S0036024421060029
26. Ya. G. Avdeev and T. E. Andreeva, Russ. J. Phys. Chem. A **96**, 425 (2022). https://doi.org/10.1134/S0036024422020030

Translated by M. Drozdova